

Electronic Transport in Expanded Liquid Mercury

Uzi Even and Joshua Jortner

Department of Chemistry, Tel-Aviv University, Tel-Aviv, Israel

(Received 16 November 1972)

We report the results of an experimental study of the electronic transport properties (Hall effect and electrical conductivity) of expanded liquid mercury in the density range 13.6–8.5 g cm⁻³ (temperature region 30–1500 °C and pressure region 1–1900 atm). From the correlation of the Hall coefficient and the conductivity, three distinct conduction regimes were identified in this one-component system: (a) the weak-scattering metallic region (13.6–11 g cm⁻³), (b) the strong-scattering metallic region (11.0–9.2 g cm⁻³), and (c) the localization regime (<9.2 g cm⁻³). Detailed information has been obtained for the formation of the pseudogap and the metal-nonmetal transition in this disordered system.

I. INTRODUCTION

Experimental studies of the electrical conductivity,^{1–6} the thermoelectric power,⁷ the Hall coefficient⁸ and the optical properties⁹ of expanded liquid metals and supercritical metal vapors are expected to elucidate the following features of electron transport in disordered systems.

(a) It will provide direct information concerning different conduction regimes in a disordered system, which are¹⁰ the weak-scattering metallic regime, the strong-scattering metallic regime, and the semiconductor regime, through which the system passes with decreasing density.

(b) It will provide information concerning the metal-nonmetal transition^{11–13} induced by density changes in a disordered one-component system. In particular it is interesting to inquire whether the metal-nonmetal transition can take place in a microscopically homogeneous system as argued by Mott,^{10–13} or is it preceded by density fluctuations which lead to electron localization in this disordered system.^{14–19} In the latter case the transition between the metallic and the semiconducting states may be fuzzy and not be exhibited by sharp “breaks” in the conductivity. From the experimental point of view it is important to establish how the transition can be specified in terms of the experimental transport data.

In view of the relatively low thermodynamic critical point of mercury^{3,20} ($T_c = 1763$ °K, $P_c = 1510$ atm), this system is best suited for the study of electrical transport in an expanded liquid metal. In spite of an impressive amount of experimental transport^{1–4,7} and optical data,⁹ a coherent physical picture for the electronic transport regimes and the nature of the metal-nonmetal transition in mercury did not emerge. We have recently presented a preliminary report^{8,21} of the measurements of the Hall effect in expanded liquid mercury, which yields direct information concerning the formation of a pseudogap^{10,12} in a disordered system. In the

present work we present a detailed report of the experimental study of the Hall effect in subcritical liquid mercury in the density range 13.6–8.6 g cm⁻³. We shall demonstrate that the combination of the Hall effect and the electrical conductivity data provides direct information concerning the different conduction regimes and the metal-nonmetal transition in a one-component disordered system.

II. CONDUCTIVITY REGIMES IN A DIVALENT LIQUID METAL

A. Introductory Remarks

When the distance between divalent atoms in a crystalline metal is continuously increased, the overlap between the electronic bands decreases, resulting in a metal-nonmetal transition.^{10–13} Thus, in the hypothetical case of drastically expanded solid, crystalline mercury, the conduction s band and the valence p band will be separated by a gap.^{12,22} In a disordered system the Van Hove singularities in the density-of-states function at the band edges are smeared out. Mott²³ and Cohen, Fritzsche, and Ovshinsky,²⁴ have suggested that in amorphous semiconductors the band edges exhibit tails in the energy region which is forbidden in the corresponding perfect crystalline solid. Thus, the gap separating the valence and the conduction band in a perfect crystalline solid semiconductor is replaced in the disordered system by a pseudogap,^{10,12,23} i.e., a minimum in the density of states near the Fermi energy. A gradual expansion of a divalent liquid metal results in the formation of a pseudogap. When the density of states in the pseudogap is relatively high (i.e., only somewhat lower than the free electron value) the states in the vicinity of the Fermi energy are delocalized, while when the density of states in that energy range is lowered, localized states will appear and the conductivity energy edge is located at higher energies. A coherent description of this physical

situation was provided by Mott,¹² who introduced a pseudogap depth parameter g relating the density of states $N(E_F)$ at the Fermi energy to the free electron (fe) value

$$g = N(E_F)/N(E_F)_{fe}. \quad (1)$$

Utilizing Anderson's model²⁵ for cellular disorder, Mott has predicted¹² that metallic conductivity occurs for

$$g \gtrsim \frac{1}{3}, \quad (2)$$

while for lower g values, localized states will appear in the pseudogap, so that the system will exhibit the features of a semiconductor.

B. Weak-Scattering Metallic Regime

The weak-scattering situation prevails when the phase-coherence length of the electron exceeds the Fermi wavelength, i. e., $\lambda k_F > 1$ where λ is the mean free path and $k_F \propto E_F^{1/2}$ corresponds to the Fermi wave number. Under these circumstances, electron transport can be handled by low-order perturbation theory. The electrical conductivity σ can be in general expressed in the form²⁶

$$\sigma = e^2 S \lambda / 12\pi^3 \hbar, \quad (3)$$

where S represents the area of the Fermi surface. It was demonstrated by Faber²⁷ that a first-order correction to the Born approximation results in $\lambda = \lambda_{fe} g^{-2}$, where the free-electron mean free path λ_{fe} is calculated by the Ziman theory,²⁸ while $S = S_{fe} g^2$. Thus, in the weak-scattering limit,

$$\sigma = e^2 S_{fe} \lambda_{fe} / 12\pi^3 \hbar, \quad (4)$$

so that the electrical conductivity is independent^{10,12} of the pseudogap depth g .

To the best of our knowledge no adequate theory has yet been provided for the Hall coefficient R and for the Hall mobility $\mu = |R|\sigma$ in the weak-scattering region. This problem was handled by Ziman^{28b} and by Fukuyama *et al.*²⁹ A plausibility argument can be provided by considering the Hall coefficient R for the free-electron case²⁶

$$R = 12\pi^3 / em^* S V_F, \quad (5)$$

where m^* is the effective mass and V_F represents the Fermi velocity. For a spherical Fermi surface one gets the conventional expression

$$R_{fe} = 1/ne. \quad (6)$$

Now, as pointed out by Ziman,^{28b} Eq. (5) was derived utilizing the conventional expression for the Lorentz force $\vec{F} = e\vec{V} \times \vec{H}$, where H is the magnetic field. It was argued¹² that when $g \neq 1$ one can apply Edward's³⁰ recipe replacing the velocity operator V_k by the current operator J_k , so that (for any

wave vector k) $eV_k \rightarrow J_k$. This substitution does not affect the electrical conductivity [Eq. (4)], while the Hall coefficient is scaled by the reciprocal pseudogap depth, so that

$$R = (1/ne)g^{-1}. \quad (7)$$

On the other hand, when the velocity operator in the Lorentz force is replaced by the current operator an additional g factor is introduced into the Hall coefficient whereupon

$$R = (1/ne)g^{-2}. \quad (8)$$

Equation (8) was obtained by Fukuyama *et al.*²³ who derived the Hall conductivity for a nearly-free-electron system utilizing many-body perturbation techniques. In conclusion, it is important to point out that in the weak scattering metallic region no direct correlation exists between the electrical conductivity and the Hall coefficient. When the liquid metal density is lowered over a small region (so that S_{fe} is practically invariant) the change in the electrical conductivity reflects the decrease in the free-electron mean free path λ_{fe} . On the other hand, deviations of the Hall coefficient from its free electron value may be tentatively assigned to changes in g .

C. Strong-Scattering Metallic Region

It was argued by Mott¹³ that the mean free path cannot be lower than the near lattice spacing a so that the strong scattering regime is specified by $\lambda = a$. Making use of Eq. (3) the conductivity takes the form

$$\sigma = (e^2 S_{fe} a / 12\pi^3 \hbar) g^2. \quad (9)$$

A tentative use²¹ of Eq. (7) for the strong-scattering region as proposed by Straub *et al.*,³¹

$$R = R_{fe} g^{-1}, \quad (10)$$

yields a direct correlation between the Hall coefficient and the pseudogap depth, and hence yields a direct relation between σ and R , i. e., $\sigma \propto (R_{fe}/R)^2$. A systematic derivation of this result was recently provided by Friedman.³² It was originally proposed by Cohen³³ and by Mott¹³ that in the strong-scattering situation, where scattering of the electron occurs on each lattice site, electron transport can be described in terms of a diffusion process, whereupon the electronic wavefunctions do not exhibit any phase correlation between different lattice sites. This model was utilized by Hindley³⁴ and by Friedman³² for the calculation of the electrical conductivity and of the Hall coefficient in a degenerate electron gas and in amorphous semiconductors.

Friedman³² has considered a tight-binding s band invoking the random-phase approximation, so that the expansion coefficients of the atomic wave func-

tions on different lattice sites have no phase correlation. Utilizing the Kubo-Greenwood formula,³⁵ the electrical conductivity and the Hall coefficient can be expressed in terms of the components of the conductivity tensor

$$\sigma = \sigma_{xx} = \frac{2\pi}{3} \left(\frac{e^2}{\hbar a} \right) Z a^6 J^2 N(E_F)^2, \quad (11a)$$

$$R = \frac{\sigma_{xy}}{\sigma_{xx}^2 H} = \frac{3\eta \bar{Z}}{Z^2 e J N(E_F)}, \quad (11b)$$

where Z is the number of nearest neighbors, \bar{Z} represents the number of triangular closed paths around each lattice site, η corresponds to a geometrical factor, J is the interatomic exchange integral between nearest neighbors (which is kept constant considering just cellular disorder), and finally a is the lattice spacing which for a liquid metal is $n = a^{-3}$. Following Mott,^{10,36} we assume that these theoretical results are applicable to the more general case of a conduction band originating from s and p overlap.

Defining an auxiliary parameter

$$X = a^3 J N(E_F), \quad (12)$$

one gets for the electrical conductivity

$$\sigma = \frac{2}{3} \pi Z (e^2 / \hbar a) X^2. \quad (13)$$

The Hall coefficient is

$$R = \frac{3\eta}{Z} \left(\frac{\bar{Z}}{Z} \right) \frac{1}{ne} X^{-1}, \quad (14)$$

while the Hall mobility μ is given by

$$\mu = \left(\frac{2\pi\eta\bar{Z}}{Z} \right) \left(\frac{ea^2}{\hbar} \right) X. \quad (15)$$

Utilizing Eqs. (13)–(15) for the strong-scattering limit we can directly relate the electrical conductivity and the Hall mobility to (R/R_{te}) , the deviation of the Hall coefficient from the free-electron value,

$$\sigma = \pi \left(\frac{\bar{Z}}{Z} \right)^2 \left(\frac{6\eta^2}{Z} \right) \left(\frac{e^2}{\hbar a} \right) \left(\frac{R_{te}}{R} \right)^2, \quad (16a)$$

$$\mu = 2\pi \left(\frac{\bar{Z}}{Z} \right)^2 \left(\frac{3\eta^2}{Z} \right) \left(\frac{ea^2}{\hbar} \right) \left(\frac{R_{te}}{R} \right). \quad (16b)$$

It is important to note that Eqs. (13)–(16) provide a general result of the Friedman model. These relations should be utilized for a quantitative test for the applicability of the strong-scattering regime.

Finally, one can establish a semiquantitative relation between the Hall coefficient and the pseudogap depth. Following Friedman^{32,36} Eq. (14) can be rewritten in the form

$$\frac{R}{R_{te}} = 4\eta F(\bar{Z}/Z) g^{-1}, \quad (17)$$

where F is the filling band factor

$$F = E_F / W \quad (17a)$$

and W is the bandwidth. In a monovalent metal $F = \frac{1}{2}$, while in divalent metal where the metallic properties originate from overlap between bands a unique determination of F is difficult but we may expect that $0.5 < F < 1.0$. Setting $\bar{Z} = Z$ and $\eta = \frac{1}{3}$, we get, from Eq. (14),

$$(R_{te}/R) = \kappa g, \quad (18)$$

where

$$0.7 < \kappa < 1.5. \quad (19)$$

Our experimental results for expanded liquid mercury indicate that $\kappa \approx 1$ for that system. It is important to point out that for a divalent liquid metal, κ is not well defined, and may exhibit a density dependence. For the sake of quantitative analysis, Eqs. (13)–(15) should be utilized.

From the foregoing discussion we conclude that in the strong scattering metallic region (a) the electrical conductivity is proportional to $(R_{te}/R)^2$, (b) the Hall mobility is proportional to R_{te}/R , and (c) the electrical conductivity can be correlated with the square of the pseudogap depth, while similarly μ is proportional to g .

D. Expanded Liquid Mercury in the Strong-Scattering Region

It will be useful to provide numerical estimates for the electrical transport properties of an expanded liquid mercury in the strong scattering situation. We shall make use of values

$$\eta = \frac{1}{3}, \quad \bar{Z} = Z.$$

The coordination number in normal liquid mercury at room temperature was determined by Rivlin *et al.*³⁷ who get

$$Z \approx 10, \quad a = 3 \text{ \AA}.$$

Invoking the assumption that these parameters are slowly varying with moderate density changes we get, from Eqs. (13)–(15),

$$\sigma = 1700 (R_{te}/R)^2 \Omega^{-1} \text{cm}^{-1}, \quad (20)$$

$$\mu = 0.28 (R_{te}/R) \text{cm}^2 \text{V}^{-1} \text{sec}^{-1}. \quad (21)$$

In order to correct these results for density changes [expressed in terms of the parameter a in Eqs. (13)–(15)], we shall define the normalized conductivity σ_n and the normalized mobility μ_n in the form

$$\sigma_n = \sigma \left(\frac{d_0}{d} \right)^{1/3} = 1700 \left(\frac{R_{te}}{R} \right)^2 \Omega^{-1} \text{cm}^{-1}, \quad (22)$$

$$\mu_n = \mu \left(\frac{d_0}{d} \right)^{-2/3} = 0.28 \left(\frac{R_{te}}{R} \right) \text{cm}^2 \text{V}^{-1} \text{sec}^{-1}, \quad (23)$$

where d_0 and d represent the mercury density at room temperature and at higher temperature and

pressure, respectively. It is expected that Eqs. (22) and (23) will be valid over all the strong-scattering regions while, when at densities below the metal-nonmetal transition the transport properties will exhibit deviations from these relations.

III. EXPERIMENTAL PROCEDURES

We have measured the Hall coefficient and the electrical conductivity of subcritical mercury over the temperature range 20–1500 °C and in the pressure range 1–2000 atm. In a separate report³⁸ we have presented a detailed account of the experimental techniques developed by us for the measurement of the Hall effect and the conductivity at elevated temperatures and pressures. The experimental setup consists of the following components³⁸:

(a) high-pressure vessel for the pressure range 1–2000 atm; (b) temperature-controlled furnace for the range 20–1500 °C; (c) a recrystallized alumina sample cell for simultaneous measurements of the Hall coefficient and of the conductivity. The dimensions of the liquid-metal sample are 15×13×0.5 mm. (d) a magnet (200-mm diam, 300-mm length, ~100-G field strength) located within the high-pressure vessel, and its ac power supply (10-kW narrow-band power amplifier); (e) Hall-current generator (10-W power amplifier, current up to 5 A); (f) Hall-voltage detection system consisting of a filter, a low-noise amplifier, a second filtering state followed by a phase-sensitive detector; (g) conductivity-measurement unit.

A block diagram of the experimental setup is portrayed in Fig. 1, while in Fig. 2 we display the electronic setup for Hall-effect measurements.

The Hall coefficient was measured by the double-ac method.^{39,40} An ac current of ~5 A at 21.6 kHz and an ac magnetic field at ~100 G at 1.6 kHz produced Hall voltages of 10⁻⁹–10⁻⁸ V (in subcritical mercury at different temperatures and pressures) at the sum and at the difference frequencies. The Hall voltage was measured at the difference frequency of 20 kHz.

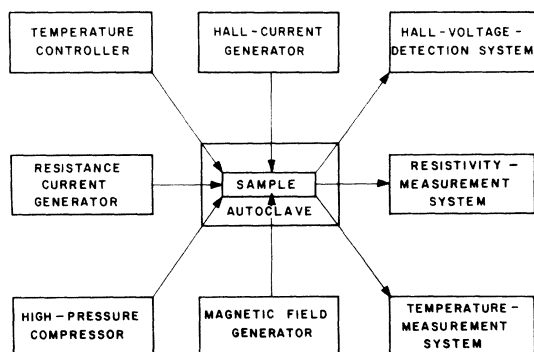


FIG. 1. Block diagram of the experimental setup.

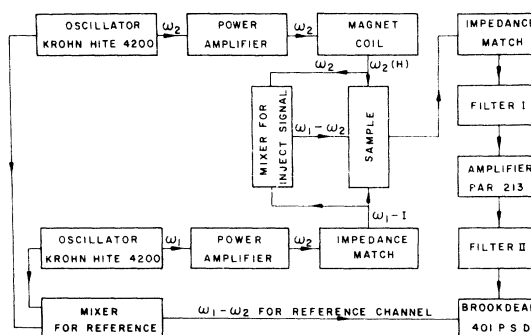


FIG. 2. Block diagram of the electronic system for double-AC Hall-effect measurements. (P. S. D. is phase-sensitive detector.)

The following tests were performed by us to check the operation of the experimental setup for Hall-effect measurements.

(a) Linearity checks of the Hall voltage as a function of the magnetic field (at a constant current) and as a function of the Hall current (at a constant magnetic field) did yield satisfactory results. This linear dependence indicates that most systematic errors in the double-ac method have been eliminated.^{39,40} To get rid of other spurious effects⁴¹ in the double-ac method, which maintain the linear dependence of the Hall voltage on the magnetic field and on the Hall current, we have (i) chosen the frequencies of the Hall current, the magnetic field, and the Hall voltage to be located well above the mechanical or the thermal frequencies characterizing the sample; (ii) maintained structural stiffness to eliminate possible motional freedom of the sample cell; (iii) devoted special attention to the linear performance of the “critical” parts of the detection system (i.e., sample electrical contacts, first filtering detection stage and preamplifier).

(b) Linearity of the Hall voltage on the cell thickness was verified.

(c) The absolute value of R at room temperature (RT), $T = 30$ °C, accounting for the finite sample size, was determined to be $R/R_{t_0} = 0.92 \pm 0.10$ [where the Hall voltage is $V_{RT} = (3.1 \pm 0.1) \times 10^{-9}$ V]. The main uncertainty in this value originates from the determination of the sample thickness. This value is within 6% of Greenfield’s⁴² result.

(d) Our results for R/R_{t_0} in the temperature region 30–300 °C are consistent with previous data.⁴²

(e) The experimental results for the Hall coefficient (and for the electrical conductivity) were identical upon heating and upon cooling of the cell.

The resistivity of mercury was measured by the four-probe method at a frequency of 10 Hz, eliminating contact-resistance errors.

The experimental accuracy of our measurements can be summarized as follows: (a) Absolute accuracy of pressure measurements in the range 1–2000 atm is ± 2 atm. (b) The temperature in the range 30–1500 °C was stabilized to within ± 0.2 °C, while the absolute determination of the temperature is accurate within $\pm 0.4\%$ (i. e., ± 6 °C at 1500 °C). (c) The absolute value of R is believed to be accurate within $\pm 10\%$, while the relative values of the Hall voltage (normalized to the room-temperature value) are obtained to better than 5%. (d) The relative resistivity (normalized to the room-temperature value) are accurate to within 2%.

IV. HALL EFFECT AND ELECTRICAL CONDUCTIVITY IN EXPANDED LIQUID MERCURY

We have measured the Hall effect and the electrical conductivity of subcritical mercury in the temperature region 20–1500 °C and in the pressure range 1–1900 atm. This region corresponds to the density range 13.6–8.5 gm cm⁻³. The density data were obtained from a recent work of Hensel *et al.*⁴³ who measured simultaneously the density and the electrical conductivity. Near the critical point a small ($\sim 0.5\%$) uncertainty in the temperature measurement leads to a considerable error in the density. In view of the uncertainty in the absolute determination of the temperature both in Hensel's measurements and in ours, we have utilized the electrical conductivity, which is determined quite accurately ($\pm 1\%$) as a common variable for comparison with Hensel's density data.⁴³ From the present simultaneous determination of the Hall coefficient and of the conductivity and from Hensel's simultaneous measurements⁴³ of the conductivity and the density we have extracted the density dependence of the Hall coefficient and of the Hall mobility. In a preliminary report⁸ we have utilized our temperature and pressure measurements to obtain the density from Hensel's equation of state data.⁴³ The present data are more detailed and more accurate than those previously reported by us.⁸

Our experimental results for the density dependence of the electrical transport properties of expanded liquid mercury are presented in Figs. 3 and 4, where we have displayed the Hall voltage V_H normalized to the room-temperature value $V_{RT} = 3.1$ nV, the Hall mobility $\mu = |R| \sigma$, the electrical conductivity and the Hall coefficient R/R_{Fe} normalized to the free-electron value.

V. ELECTRONIC TRANSPORT IN EXPANDED LIQUID MERCURY

On the basis of our combined Hall effect and conductivity data we can distinguish three distinct conduction regimes in expanded liquid mercury.

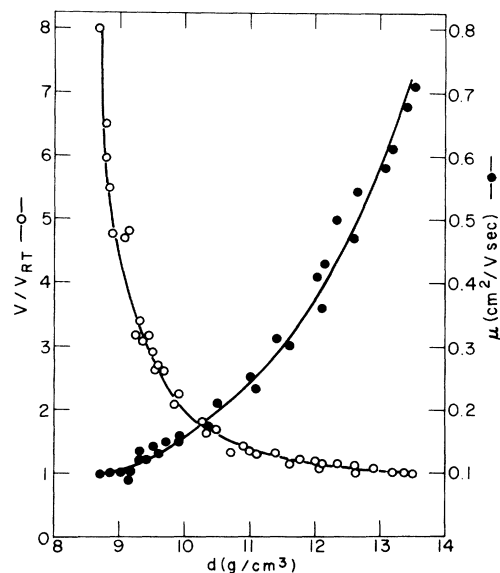


FIG. 3. Density dependence of the Hall voltage V (normalized to the room temperature value V_{RT}) and of the Hall mobility in expanded liquid mercury.

a. Weak-scattering regime ($11.0 < d < 13.6$ gm cm⁻³). In this region the transport properties of liquid mercury are amenable to theoretical description in terms of the free electron model. The high conductivity can be handled by Ziman's theory,¹² which can be recast in the form of Eq. (4), where the mean free path (or the scattering time) can be expressed in terms of the Born approximation, utilizing the pseudopotential proposed by Evans.⁴⁴ The mean free path thus obtained is $\lambda \approx 3a = 7$ Å and the self-consistency condition for the applicability of the weak-scattering picture is satisfied.

No good theory is as yet available for the Hall coefficient in the weak-scattering regime. If Ziman's equation (7) or alternatively Eq. (8) are to be believed, then our experimental results $R/R_{Fe} = 1$ imply that $g = 1$ in this regime. The calculations of the density of states for normal liquid mercury by Evans⁴⁴ and by Chan and Ballantine⁴⁵ indicate that at $d = 13.6$ gm cm⁻³, $g \approx 0.9 - 1.0$.

The decrease of the electrical conductivity over the weak-scattering regime (accompanied by a parallel decrease in μ) reflects the decrease of the mean free path from $\lambda = 7$ Å $\approx 3a$ at $d = 13.6$ gm cm⁻³ to $\lambda = 2$ Å $\approx a$ at $d = 11.0$ gm cm⁻³. At the lower-density limit of the weak-scattering regime, $\lambda = a$. The basic condition for the applicability of the weak-scattering model $k_F \lambda \gg 1$ (where $k_F \propto E_F^{1/2} = 1.16$ Å⁻¹ the Fermi wave number) breaks down for $d = 11.0$ gm cm⁻³, where $\lambda k_F = 2.3$. Thus, the density $d = 11.0$ gm cm⁻³ represents the onset of the strong-scattering regime.

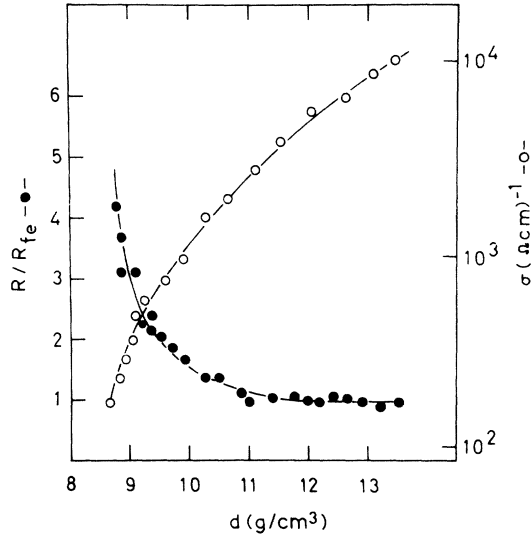


FIG. 4. Density dependence of the Hall coefficient (normalized to the free-electron value) and of the electrical conductivity in expanded liquid mercury.

b. Strong scattering regime ($9.2 < d < 11.0 \text{ g cm}^{-3}$). The identification of this regime rests on the following qualitative arguments: (a) The change of the conductivity ($300\text{--}3000 \text{ } \Omega^{-1} \text{ cm}^{-1}$) in this density region is consistent with Mott's general arguments^{10,12} for the magnitude of the conductivity in the strong scattering regime. (b) The positive deviations of R/R_{fe} from the free-electron value are consistent with the tentative use of Eq. (10) or the more elaborate result of Friedman's theory³² [Eqs. (16) and (18)]. In Fig. 5 we present the density dependence of g in the strong-scattering region. It should be stressed that g is temperature

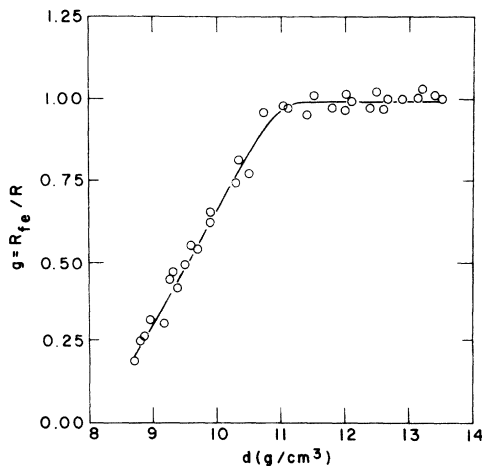


FIG. 5. Density dependence of the pseudogap depth parameter obtained from Hall-effect data in expanded liquid mercury.

independent at constant density, as expected.

(c) A qualitative correlation of the electrical transport properties indicates that in this density range σ decreases by a factor of ~ 8 , R/R_{fe} increases by a factor of ~ 3 , while μ decreases by a factor of ~ 2.5 . This behavior is consistent with the functional dependence [see Eqs. (12)–(16)], $\sigma \propto (R_{fe}/R)^2$, and $\mu \propto (R_{fe}/R)$. Utilizing Eq. (17), we have $\sigma \propto g^2$, $(R/R_{fe}) \propto g^{-1}$, and $\mu \propto g$, where g varies in the range $g = 1.0\text{--}0.3$ (see Fig. 5).

Detailed quantitative physical information concerning the strong-scattering regime is obtained by utilizing our results to test Friedman's random-phase approximation.¹⁹ Making use of Eqs. (13)–(15), we plot in Figs. 6 and 7 the normalized conductivity and the normalized mobility vs R_{fe}/R . In the density range $11.0\text{--}9.2 \text{ g cm}^{-3}$ the following experimental correlations hold:

$$\sigma_n = 2600 (R_{fe}/R)^2 \text{ } \Omega^{-1} \text{ cm}^{-1},$$

$$\mu_n = 0.24 (R_{fe}/R) \text{ cm}^2 \text{ V}^{-1} \text{ sec}^{-1}.$$

These experimental relations are in excellent quantitative agreement with the theoretical predictions given by Eqs. (22) and (23).

We conclude with the following comments: (a) Figures 6 and 7 clearly exhibit the onset and the termination of the strong-scattering regime. These data are obtained from the correlation of two trans-

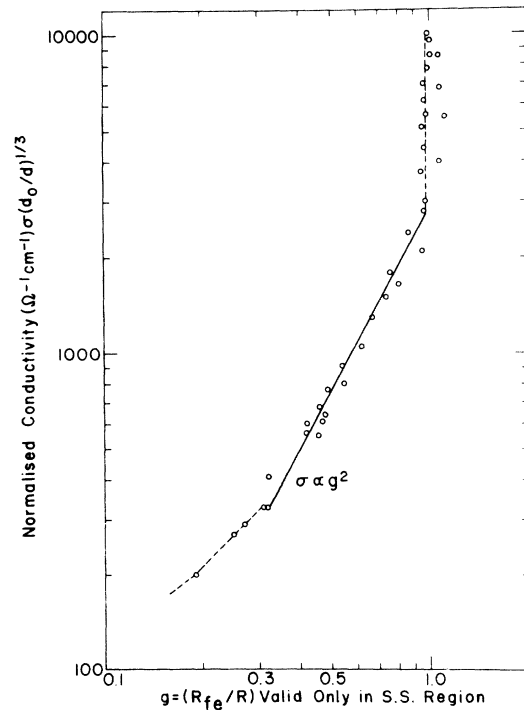


FIG. 6. Dependence of the normalized conductivity on the pseudogap depth parameter in the strong-scattering regime.

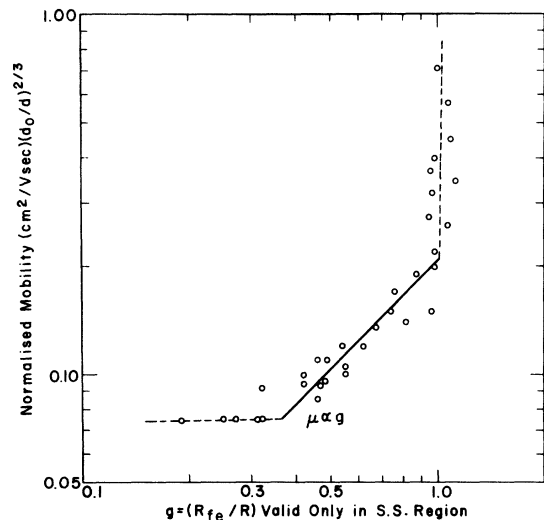


FIG. 7. Dependence of the normalized mobility on the pseudogap depth parameter in the strong-scattering regime.

port properties (σ and R) and cannot be obtained from "breaks" in the conductivity alone. (b) The lower density limit for the strong-scattering regime ($d = 9.2 \text{ g cm}^{-3}$) corresponds to $g = 0.32$. The critical $g = 0.32$ value for the termination of the strong-scattering regime is in excellent agreement with Mott's theoretical prediction for the onset of localized states and semiconducting behavior at $g \approx \frac{1}{3}$.

c. *Localization region* ($d < 9.2 \text{ g cm}^{-3}$). Here the electrical conductivity $\sigma < 300 (\Omega \text{ cm})^{-1}$ and the Hall coefficient exhibit strong density dependence, while the mobility is practically constant. The Friedman theory for the strong-scattering regime [Eqs. (12)–(16)] breaks down at $d \leq 9.2 \text{ g cm}^{-3}$. In this region, where $g < \frac{1}{3}$, localized states are expected to appear in the pseudogap near the Fermi energy. The appearance of such localized states in this disordered system implies semiconducting behavior, whereupon electron transport will be governed by thermal excitations above the conduction edge. Supporting physical information for the semiconducting nature of expanded liquid mercury in the density region $d < 9.2 \text{ g cm}^{-3}$ is obtained from the following experimental data.

(a) The slow variation of the mobility μ over the density region $9.2\text{--}8.5 \text{ g cm}^{-3}$ may be reminiscent of the behavior of liquid semiconductors, where μ is expected to be temperature independent, while the electrical conductivity and the Hall coefficient exhibit temperature dependence.

(b) The density dependence (at constant temperature) and the temperature coefficients of the electrical conductivity, as recorded by Schmutzler,⁴⁶ exhibit a sharp increase at $d < 9 \text{ g cm}^{-3}$, indicating

the onset of activated transport.

(c) From the correlation between the thermopower S and the electrical conductivity for the semiconductor region $\ln(\sigma/\sigma_0) = (1 - eS/K_B)$ Schmutzler⁴⁶ has demonstrated that the onset of the semiconducting behaviors occurs for $d < 7.8 \text{ g cm}^{-3}$.

Finally, we would like to point out a rather serious disagreement between our value of $d = 9.2 \text{ g cm}^{-3}$ for the onset of localized states and the value of $d = 5.5 \text{ g cm}^{-3}$ estimated by Hensel from his optical data.⁹ This discrepancy probably originates from the extrapolation procedure employed by Hensel.⁹

VI. BRIEF COMMENTS ON THE INAPPLICABILITY OF PERCOLATION THEORY FOR THE DENSITY RANGE $11.0\text{--}9.2 \text{ g cm}^{-3}$

The question of the relation between the localization problem in disordered systems and classical percolation theory was first considered by Ziman¹⁴ and later elaborated on by Zallen and Scher.¹⁵ Cohen *et al.*^{16–19} have studied transport in disordered systems in terms of lattice percolation theory. Recently, Kirkpatrick⁴⁷ has provided a detailed theoretical study of band percolation in a three-dimensional lattice presenting both analytical results based on the effective medium theory and numerical data for the electrical conductivity. This approach considers an inhomogeneous medium, with an allowed fraction of conducting regions for electrons at the Fermi energy. Let p be the fraction of allowed volume; then according to Kirkpatrick the electrical conductivity is⁴⁷

$$\sigma \propto \frac{3}{2}(p - \frac{1}{3}), \quad 1 > p \geq 0.4 \quad (24a)$$

$$\sigma \propto (p - p_c)^{8/5}, \quad p_c < p < 0.4 \quad (24b)$$

$$\sigma = 0, \quad p < p_c \quad (24c)$$

p_c is the percolation threshold which is estimated numerically to be ≈ 0.2 .

Concerning the Hall coefficient for the percolation problem, Juretschke and Landauer⁴⁸ have claimed that $R_{H0}/R = p$ for relatively large- p values, while recently Kirkpatrick⁴⁹ has argued that

$$R_{H0}/R = P(p), \quad (25)$$

where $P(p)$ is the percolation probability (i. e., fraction of allowed nonisolated volume for electron transport), which according to numerical calculations is given by⁵⁰

$$P(p) = P, \quad p > 0.4 \quad (26a)$$

$$P(p) \approx 1 - e^{-25(p-0.3)}, \quad p < 0.4 \quad (26b)$$

Kirkpatrick has argued⁴⁹ that our experimental electronic transport data in the density region $d = 11.0\text{--}8.5 \text{ g cm}^{-3}$ in mercury can be interpreted on the basis of percolation theory. This suggestion drastically differs from our interpretation of

the transport data in the density region 11.0–9.2 g cm⁻³, where we visualize electron conduction in the strong scattering regime (see Secs. II and IV) to proceed in a medium which is microscopically homogeneous for electron transport.

A detailed reevaluation of our experimental data leads us to the conclusion that Kirkpatrick's percolation model is inadequate for the transport data in the density region 11.0–9.2 g cm⁻³ because of the following reasons.

(a) Utilizing Eqs. (25) and (26) to evaluate p we have replotted our conductivity data according to the predictions of the effective medium theory (Fig. 8). Systematic deviations are exhibited from the linear plot, which is predicted by Eq. (24). A better fit is obtained for the strong-scattering model. This result provides a supporting argument favoring the homogeneous strong-scattering picture.

(b) Kirkpatrick's arguments predict that the Hall mobility will exhibit a weak dependence on p in the range $0.5 < p < 1.0$, possibly tending to fall off for $p < 0.5$, as from Eqs. (24)–(26) one has^{47,51}

$$\mu \propto (3/2ne)(1 - 1/3p). \quad (27)$$

In Fig. 9 we present the values of the product μd according to Eq. (27), and compare them with the prediction of the strong-scattering theory. Again the fit to Friedman's theory is superior.

(c) The percolation concepts in a one-component system where no covalent binding effects are operative, may be applicable only provided that density fluctuations lead to microscopic inhomogeneity. A recent unpublished estimate by Cohen and Jortner of thermodynamic fluctuations in subcritical and

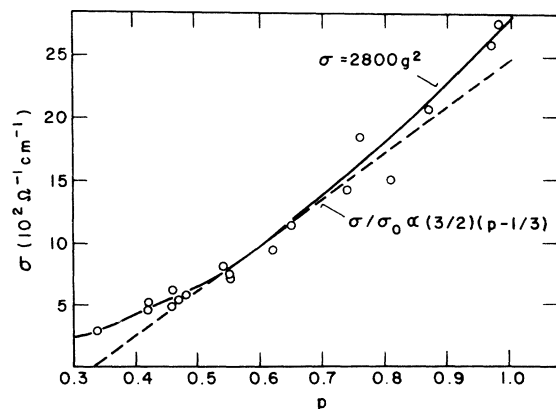


FIG. 8. Attempt to fit the mercury conductivity data in the density range $d = 11.0$ – 9.2 g cm⁻³ to Kirkpatrick's percolation theory. Dashed line represents the prediction of effective-medium theory [Eq. (24a)] while the solid line represents the prediction for the strong-scattering homogenous model preferred by us.

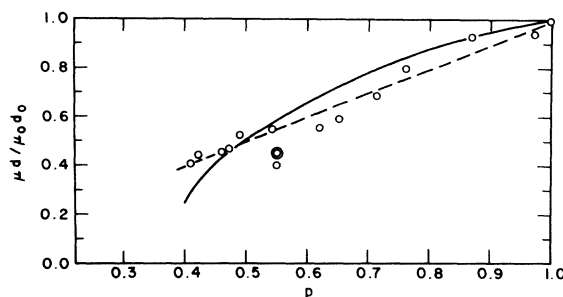


FIG. 9. Attempt to fit the mercury Hall-mobility data to percolation theory, where the solid line represents Kirkpatrick's result [Eq. (27)], while the dashed line corresponds to the strong-scattering situation.

supercritical mercury utilizing the equation-of-states data of Hensel,⁴³ indicates that for $d > 9.5$ g cm⁻³ the correlation length of the density fluctuations is smaller than the interatomic spacing. Thus in the density range 11.0–9.2 g cm⁻³ electron transport in this system is expected to proceed in a homogeneous medium.

VII. DISCUSSION

In this paper we have demonstrated the applicability of combined Hall-effect and conductivity data to yield the following physical information concerning electron transport and the metal-non-metal transition in a disordered one-component system.

(a) Two metallic conductivity regimes were unambiguously identified in expanded liquid mercury.

(b) The transition density between the weak scattering and the strong-scattering metallic regimes is specified in terms of the following observables: (i) onset of deviations of (R/R_{te}) from the free-electron value; (ii) $\sigma \approx 2800 \Omega^{-1}$ in agreement with Mott's predictions^{10,12,13,23}; (iii) onset of the relations $\sigma \propto (R_{te}/R)^2$ and $\mu \propto (R_{te}/R)$.

(c) The termination of the strong scattering regime occurs at $d = 9.2$ g cm⁻³. This density is characterized by the following features: (i) $g \approx 0.32$; (ii) $\sigma = 270 \Omega^{-1} \text{cm}^{-1}$, which are in perfect agreement with Mott's arguments concerning the onset of localization in a disordered system.^{10,12} Thus, the density range $d < 9.2$ g cm⁻³ is assigned by us to correspond to the localization regime. This conclusion is supported by the onset of a substantial temperature dependence of the electrical conductivity at about $d < 9$ g cm⁻³. One should, however, note that from the correlation between the electrical conductivity and the thermoelectric power data we concur with Schmutzler and Hensel⁴⁶ that semiconductor behavior is encountered in the density range $d < 7.8$ g cm⁻³. The behavior of expanded liquid mercury in the density range 9.2–

7.8 g cm^{-3} is not well understood. Two extreme possibilities may be considered: (i) localized states near the Fermi energy set in at 9.2 g cm^{-3} as predicted by Mott, while only at $d \lesssim 7.8 \text{ g cm}^{-3}$ the energy gap between the Fermi energy and the conduction edge is $4k_B T$, manifesting itself in the thermopower-conductivity relation; (ii) the density range $7.8 < d < 9.2 \text{ g cm}^{-3}$ characterizes a continuous metal-semiconductor transition region. Thus, in all fairness we have to assert that on the basis of the electrical transport and thermoelectric power data we cannot ascertain whether the metal-nonmetal transition is sharp (occurring at 9.2 g cm^{-3}) or fuzzy (taking place in the density region $d = 9.2 \text{ g cm}^{-3}$ to $d \gtrsim 7.8 \text{ g cm}^{-3}$). For the time being, in the absence of further theoretical work on the subject, we prefer to adopt Mott's picture and to assign the onset of localization, i. e., the metal-nonmetal transition, to occur at $d = 9.2 \text{ g cm}^{-3}$.

(d) The critical density for metal-nonmetal transition in expanded liquid mercury assigned by us ($d_{CM} = 9.2 \text{ g cm}^{-3}$) considerably exceeds the thermodynamic critical density ($d_{CT} = 4.5 \text{ g cm}^{-3}$). There is no correlation between d_{CM} and d_{CT} in contrast to some theoretical conjectures.

(e) The high value of $d_{CM} = 9.2 \text{ g cm}^{-3}$ in liquid mercury can be rationalized for in terms of the

large energy gap (6 eV) between the *s* and *p* atomic states of Hg. Thus large exchange integrals (and consequently high densities) are required for sufficient interband overlap. On the other hand, the critical density for metal-nonmetal transition for Cs vapor⁵ is considerably lower ($d_{CM} = 0.45 \text{ g cm}^{-3}$). In the Cs system, spin pairing, resulting in the formation of diatomic Cs_2 molecules, may take place. If this conjecture will be supported by experimental paramagnetic susceptibility data then the physical situation in dense alkali fluids will be reminiscent of spin pairing in concentrated metal-ammonia solutions.⁵¹ The metal-nonmetal transition in the cesium system will then occur via overlap of the Σg and Σu bands of the diatomic molecule. The level spacing⁵² of the molecular Σg and Σu states in Cs_2 is approximately 1 eV, so that the metal-nonmetal transition in this system will occur at considerably lower density as compared to the case of expanded mercury.

ACKNOWLEDGMENTS

We are grateful to Professor N. F. Mott F.R.S., Professor M. H. Cohen, and Dr. F. Hensel for stimulating discussions, and to Dr. S. Kirkpatrick for interesting correspondence. We wish to thank M. Levine and J. Magen for their competent technical assistance.

- ¹D. R. Postill, R. G. Ross, and N. E. Cusack, *Phil. Mag.* **18**, 519 (1968).
- ²I. K. Kikoin, A. P. Senchenkov, E. V. Gelman, M. M. Korsunskiy, and U. S. P. Naurzakov, *Soviet Phys. JETP* **22**, 89 (1966).
- ³E. U. Franck and F. Hensel, *Phys. Rev.* **147**, 109 (1967).
- ⁴E. U. Franck and F. Hensel, *Rev. Mod. Phys.* **40**, 697 (1968).
- ⁵H. Renkert, thesis (University of Karlsruhe, 1969) (unpublished).
- ⁶W. F. Freyland and F. Hensel, *Ber. Bunsenges Phys. Chem.* **76**, 347 (1972).
- ⁷R. W. Schmutzler and F. Hensel, *Ber. Bunsenges Phys. Chem.* **76**, (1972).
- ⁸U. Even and J. Jortner, *Phys. Rev. Letters* **28**, 31 (1972).
- ⁹F. Hensel, *Phys. Letters* **31**, 88 (1970).
- ¹⁰N. F. Mott, *Phil. Mag.* **24**, 1 (1971).
- ¹¹N. F. Mott, *Phil. Mag.* **6**, 287 (1961).
- ¹²N. F. Mott, *Phil. Mag.* **13**, 989 (1966).
- ¹³N. F. Mott, *Adv. Phys.* **16**, 49 (1967).
- ¹⁴J. M. Ziman, *J. Phys. C* **1**, 1532 (1968).
- ¹⁵R. Zallen and H. Scher, *Phys. Rev. B* **4**, 4471 (1971).
- ¹⁶M. H. Cohen, *Proceedings of the Tenth International Conference on the Physics of Semiconductors, Cambridge, Mass.* (U. S. Atomic Energy Commission, Oak Ridge, Tenn., 1970), p. 645.
- ¹⁷(a) T. P. Eggarter and M. H. Cohen, *Phys. Rev. Letters* **25**, 807 (1970); (b) *Phys. Rev. Letters* **27**, 129 (1971).
- ¹⁸E. N. Economou, S. Kirkpatrick, M. H. Cohen, and T. P. Eggarter, *Phys. Rev. Letters* **25**, 520 (1970).
- ¹⁹M. H. Cohen and J. Sak, *J. Non-crystalline Solids* **8-10**, 696 (1972).
- ²⁰F. Birch, *Phys. Rev.* **41**, 641 (1932).
- ²¹U. Even and J. Jortner, *Phil. Mag.* **25**, 715 (1972).
- ²²A. H. Wilson, *Proc. Roy. Soc. A* **133**, 458 (1931).
- ²³N. F. Mott, *Phil. Mag.* **17**, 1259 (1968).
- ²⁴M. H. Cohen, H. Fritzschke, and S. R. Ovshinsky, *Phys. Rev. Letters* **22**, 1065 (1969).
- ²⁵P. W. Anderson, *Phys. Rev.* **109**, 1492 (1958).
- ²⁶J. M. Ziman, *Electron and Phonons* (Oxford U. P., London, 1960).
- ²⁷T. E. Faber, *Adv. Phys.* **15**, 547 (1966).
- ²⁸(a) J. M. Ziman, *Phil. Mag.* **6**, 1013 (1961); (b) *Adv. Phys.* **16**, 578 (1967).
- ²⁹H. Fukuyama, H. Ebisawa, and J. Wada, *Prog. Theoret. Phys.* **42**, 497 (1968).
- ³⁰S. F. Edwards, *Phil. Mag.* **3**, 1020 (1958).
- ³¹W. I. Straub, H. Roth, W. Bernard, S. Goldstein, and J. E. Mulkern, *Phys. Rev. Letters* **21**, 752 (1968).
- ³²L. Friedman, *J. Non-crystalline Solids* **6**, 329 (1971).
- ³³M. H. Cohen, *Proceedings of the Symposium on Semiconductor Effects in Amorphous Solids* (North-Holland, Amsterdam, 1970).
- ³⁴N. K. Hindley, *J. Non-crystalline Solids* **5**, 17 (1970).
- ³⁵R. Kubo, *J. Phys. Soc. Japan* **12**, No. 6 (1957).
- ³⁶N. F. Mott and L. Friedman, *J. Non-crystalline Solids* **7**, 103 (1972).
- ³⁷V. G. Rivlin, R. M. Waghorne, and G. I. Williams, *Phil. Mag.* **13**, 1169 (1970).
- ³⁸U. Even, M. Levine, J. Magen, and J. Jortner, *J. Appl. Phys.* (to be published).

- ³⁹E. H. Putley, *The Hall Effect and Related Phenomena* (Butterworth, London, 1960).
- ⁴⁰J. P. Jan, *Solid State Physics* (Academic, New York, 1957), Vol. 5, p. 1.
- ⁴¹H. L. McKinsie and D. Tannhauser, *J. Appl. Phys.* 40, 4954 (1969).
- ⁴²A. J. Greenfield, *Phys. Rev.* 135, A1589 (1964).
- ⁴³F. Hensel and R. W. Schmutzler, *J. Non-crystalline Solids* 8-10, 718 (1972).
- ⁴⁴R. Evans, *J. Phys. C* 2, 5137 (1970).
- ⁴⁵T. Chan and I. E. Ballantine, *Can. J. Phys.* 50, 813 (1972).
- ⁴⁶R. W. Schmutzler, Doctoral thesis (Karlsruhe University, Germany, 1971) (unpublished).
- ⁴⁷S. Kirkpatrick, *Phys. Rev. Letters* 27, 1722 (1971).
- ⁴⁸H. J. Juretschke, R. Landauer, and J. A. Swanson, *J. Appl. Phys.* 27, 838 (1956).
- ⁴⁹S. Kirkpatrick, *Proceedings of the Second International Conference on Liquid Metals, Tokyo, 1972* (Taylor and Francis, London, to be published); and private communication.
- ⁵⁰H. L. Firsch, J. Hammersley, and D. J. A. Welsh, *Phys. Rev.* 126, 949 (1962).
- ⁵¹M. H. Cohen and J. C. Thompson, *Adv. Phys.* 17, 857 (1968).
- ⁵²G. Herzberg, *Spectra of Diatomic Molecules* (Van Nostrand, New York, 1953).